Evaluation of Seals for High-Performance Cryogenic Turbomachines

R.C. Hendricks
Lewis Research Center
Cleveland, Ohio

L.T. Tam
CHAM
Huntsville, Alabama

M.J. Braun
The University of Akron
Akron, Ohio

B.L. Vlcek
Rensselaer Polytechnic Institute
Troy, New York

NASA

EVALUATION OF SEALS FOR HIGH-PERFORMANCE CRYOGENIC TURBOMACHINES

R.C. HENDRICKS
NASA Lewis Research Center
Cleveland, Ohio 44135 (USA)

L.T. TAM
CHAM
Huntsville, Alabama 35816 (USA)

M.J. BRAUN
The University of Akron
Akron, Ohio 44325 (USA)

B.L. VLCEK
Rensselaer Polytechnic Institute
Troy, New York 12180 (USA)

SUMMARY

Une approche pour calculer l'ecoulement uniforme et les characteristiques dynamique des fermetures etanchs et des paliers est discuter. La velocitee moyenne locale est tres affectais par les effets d'entree et de sortie et l'injection liquide, ce qui cause des ecoulements secondaires. Pour les maquettes en trois dimension considerez, les resultats integrales moyens etait en accord avec les resultats d'analyse. Les mesurements de pression en direction uniques n'etait pas suffisant pour donnes les variations d'ecoulement. Mai, pour les correlations de fuites d'etanches et de paliers, les principes d'etats de correspondence etait utiles. Les trois phenomenes trouvait pendant les epreuves de trois configurations de fermeture etanche excentrique sans rotation pour le "Space Shuttle Main Engine" (SSME) programme sont aussi discutez. L'injection des fluides, callages de fermeture etanche, et profile de pression sont examiner en relation au zones d'ecoulement secondaires de separation et de rigidite.

1. INTRODUCTION

Although the primary function of a seal is to control leakage, a secondary but equally important purpose is to provide dynamic stability. A seal or bearing properly designed by using computational fluid dynamics and knowledge-based methodologies can enhance turbomachine stability.

Much of the current research on seal- or bearing-driven instabilities in turbomachines is contained in NASA CP's 2133, 2238, 2250, 2443, and 2409 (refs. 1 and 2). Topics such as seal dynamic coefficients (as measured by Childs, Benckert, and Iwatsubo), analytical methods (Fleming, Nelson, Black, Brown, Muszynska, and Bently), numerical techniques (CHAM, Rhode, and Nordmann), and practical applications (gas injection and swirl brakes) are but a sampling of the research efforts of the past decade. Leakage rates for cylindrical and tapered seals can be predicted reasonably well, but direct stiffness predictions are not very accurate as revealed by a comparison with noncryogenic data (ref. 3). Tests with nonrotating convergent tapered seals revealed a rapid dropoff in direct stiffness for inlet/exit area ratios greater than 2 (ref. 4). Parallel or series hydrostatic bearings and magnetic bearings

appear to have potential for high DN and dynamic applications, but stability and longevity remain as problems (refs. 1, 2, and 5).

Herein we outline a relativistic method to calculate flow and dynamic characteristics for seals or bearings and compare this solution method with selected data of Childs (ref. 3). We also discuss leakage rates and relations between pressure profile data for three eccentric nonrotating seal tests, associated configurations, and corresponding states.

2. NUMERICAL APPROACH

Consider a shaft at a static eccentricity a and a dynamic eccentricity d rotating clockwise within a static housing (fig. 1). Such a configuration can represent a seal or a bearing. The axial pressure drop for the bearing is quite small, but for the seal it is large and engenders significant Coriolis and centrifugal forces at the inlet or convergent/divergent zones.

The problem here is that we are dealing with nonconventional flow fields in very narrow passages with the passage geometry changing periodically with time. But in order to simulate seal or bearing flows, the coordinate system must be transformed into the relativistic frame such that the geometry is invarient in time (refs. 6 and 7).

To an observer in the rotating frame the relation between absolute, relative, and grid velocity becomes

$$\underset{\sim}{U}_{abs} = \left.\frac{d\underset{\sim}{r}}{dt}\right|_{rot} + \underset{\sim}{\omega} \times \underset{\sim}{r} = \underset{\sim}{U} \quad + \quad \underset{\sim}{\omega} \times \underset{\sim}{r} \tag{1}$$

$$\begin{array}{ccc} \text{Absolute} = & \text{Relative} & \text{Grid} \\ \text{velocity} & \text{velocity} & \text{velocity} \end{array}$$

or

$$\underset{\sim}{U} = \underset{\sim}{U}_{abs} - \underset{\sim}{U}_{grid} \tag{2}$$

The accelerations become

$$\left.\frac{d\underset{\sim}{U}_{abs}}{dt}\right|_{fixed} = \left.\frac{d\underset{\sim}{U}_{abs}}{dt}\right|_{rot} + \underset{\sim}{\omega} \times \underset{\sim}{U}_{abs} \tag{3}$$

$$\left.\frac{d\underset{\sim}{U}_{abs}}{dt}\right|_{fixed} = \left.\frac{d(\underset{\sim}{U} + \underset{\sim}{\omega} \times \underset{\sim}{r})}{dt}\right|_{rot} + \underset{\sim}{\omega} \times (\underset{\sim}{U} + \underset{\sim}{\omega} \times \underset{\sim}{r}) \tag{4}$$

$$\left.\frac{d\underset{\sim}{U}_{abs}}{dt}\right|_{fixed} = \left.\frac{d\underset{\sim}{U}}{dt}\right|_{rot} + \quad 2\underset{\sim}{\omega} \times \underset{\sim}{U} \quad + \quad \underset{\sim}{\omega} \times (\underset{\sim}{\omega} \times \underset{\sim}{r}) \tag{5}$$

$$\begin{array}{ccccc} \text{Absolute} & = & \text{Relative} & + & \text{Coriolis} & + & \text{Centrifugal} \\ \text{acceleration} & & \text{acceleration} & & \text{acceleration} & & \text{acceleration} \end{array}$$

where eq. (5) is for constant $\underset{\sim}{\omega}$. The resulting equation of motion becomes

$$\rho \left.\frac{D\underset{\sim}{U}}{Dt}\right|_{rot} + 2\rho\underset{\sim}{\omega} \times \underset{\sim}{U} + \rho\underset{\sim}{\omega} \times (\underset{\sim}{\omega} \times \underset{\sim}{r}) = -\nabla p - \nabla : \underset{\approx}{\tau} + \rho g \tag{6}$$

Expanding this form of the Navier-Stokes equations gives rise to two source terms to be added to the existing cylindrical polar numerical code. These source terms for the U and V momentum equations become

$$S(U) = -2\rho\omega V Vol_{cell} \tag{7}$$

$$S(V) = (\rho\omega^2 r + 2\rho\omega U)Vol_{cell} \tag{8}$$

The turbulent flow in a seal is simulated by way of the Prandtl mixing-length model. The mixing length ℓ_m is characterized as

$$\begin{aligned}
\frac{y}{\delta} \leq \frac{\lambda}{K} \quad & \left.\frac{\ell_m}{\delta}\right. = K\frac{y}{\delta} \qquad K = 0.435 \\
\frac{y}{\delta} > \frac{\lambda}{K} \quad & \left.\frac{\ell_m}{\delta}\right. = \lambda \qquad \lambda = 0.09
\end{aligned} \tag{9}$$

where δ is the normal distance measured between the stator and the rotor surface and y is the minimum local distance measured from the stator and the rotor surfaces.

The resulting Navier-Stokes equations describe the time-averaged distributions of velocity, pressure, etc. Note that the stress tensor described earlier now also contains Reynolds stress terms $-\rho\overline{u_i'u_j'}$. The turbulence model currently used in our seal flow simulation makes use of the eddy-viscosity concept to compute the Reynolds stresses from

$$-\rho\overline{u_i'u_j'} = \mu_t \left(\frac{du_i}{dx_j} + \frac{du_j}{dx_i} - \frac{2}{3} \underset{\sim}{\nabla} \cdot \underset{\sim}{U} \delta_{ij} \right) \tag{10}$$

where δ_{ij} is the Kronecker operator, $\mu_t = \rho\ell_m^2\varphi$ is the eddy viscosity with ℓ_m the mixing length, and φ is the rate of strain.

If we define the effective viscosity as $\mu_{eff} = \mu_l + \mu_t$, the stress tensor $\nabla(\tau_{ij} - \rho\overline{u_i'u_j'})$ can be simply replaced by $\nabla(\tau_{eff})$. The shaft reaction forces are

$$\text{Radial:} \qquad F_r = -\int_0^{2\pi} \int_0^1 \rho \cos\varphi \, r_i \, d\varphi \, dz \tag{11}$$

$$\text{Tangential:} \qquad F_\theta = -\int_0^{2\pi} \int_0^1 \rho \sin\varphi \, r_i \, d\varphi \, dz \tag{12}$$

Further, in the numerical approach the shaft rotates clockwise, and the tangential force F_θ would be defined by $-F_\theta$. Stiffness is then related to the ratio F_r/clearance, and damping is related to the slope of the F_θ/clearance-versus-rotational-speed locus. The application of these equations to seal data is discussed later. For purposes of the discussion $\omega = \Omega$.

3. DISCUSSION

Figures 2 and 3 present the distribution of radial and tangential forces as a function of rotational speed for the experimental data of Childs (ref. 3) and that calculated numerically. Although there were three steps within the length of the experimental seal and the modeled seal was considered as straight cylindrical, without inlet preswirl, experiment and calculations agreed reasonably well. The calculated radial forces increased with speed but did not exhibit the positive values of the experimental data at elevated rotor speed. The omission of the internal steps or preswirl may account for this discrepancy. The tangential forces $-F_\theta$ increased with rotational speed and agreed reasonably well with the data of Childs (ref. 3).

The discussion now centers on three phenomena associated with three different fully eccentric nonrotating seal configurations.

First, helium was injected into a nonrotating straight cylindrical seal at the -90°, 0°, and 90° positions at approximately 0.8 of the seal length (fig. 4(a)). The overall magnitude of the pressure over the surface at the 0° position increased, but the magnitude over the surface at 180° decreased (fig. 4(b)). Such profiles are similar to those for an eccentric rotor; thus the injected fluid essentially functioned as an eccentric rotor. We think that the velocity patterns moved in a circumferential manner and that for fluids the injection engenders two-phase flow. Such patterns would indicate that injection direction is critical. Injection opposite to the direction of rotation would enhance stability; injection in the direction of rotation would be destabilizing. This dynamic stabilizing technique could be applied to bearings or seals (refs. 1 and 2).

The second phenomenon was found in the second step of a nonrotating three-step seal (fig. 5(a)) where the third step was choked in the 180° position. Within the first step the pressure profile at the 0° position was larger than that for the 180° position. However, within the second step the profiles crossed over (fig. 5(b)). We think that the flow at the 180° position was partially blocked by the two-phase choke at the entry to the third step and was diverted toward the 0° position. The flow was then rediverted within the third step toward the 180° position, and the pressure profile mimicked that of a diffuser (i.e., there was a monotone <u>increase</u> of pressure with axial position).

Such fluid jetting was also found to exist in single and sequential orifice and Borda inlets. It was assumed that liquidlike behavior produced fluid jetting but that data exhibiting gaslike behavior were produced by the strong separation effects (refs. 8 and 9). Fluid velocities for liquids with high subcooling fluid velocities can exceed the local sonic velocity and remain "supersonic" to 105 L/D. With proper care a seal could be designed to provide for such separations and thus enhance both stability and leakage control. However, the effect of shaft rotation on jetting zones is yet to be determined.

The third phenomenon was found within the steps of a three-step labyrinth seal of 12, 11, and 10 teeth, respectively, (fig. 6(a)). The carryover increased with axial position; so although the pressure difference between 0° and 180° was positive at the inlet, it became negative at the exit for each step (fig. 6(b)). Such crossovers in the pressure profiles provided positive and negative direct stiffness within each step with little or no resultant stiffness.

It is evident from previous discussion that fluid conditions at the inlet and exit can create zones of secondary flows that either enhance or diminish the average fluid velocity. Further, for the eccentric nonrotating tests discussed herein the pressure measurements were taken at 0° and 180° along the axial length, but these positions may not represent maximimum-to-minimum pressure variations. For example, when eccentric seals or bearings rotate at high speeds, the maximum and minimum pressures may be quite close geometrically. This points out the need for careful instrumentation guided by three-dimensional computations, data, and intuition.

4. KEY TO STABILITY

The key to stability is the average velocity profile. As the local average velocity within the bearing or seal decreases, the cross-coupled terms that contribute to instability are decreased (ref. 10). However, the increase in damping that is associated with decreases in the cross-coupled terms usually effects a decrease in direct stiffness. Thus one must consider system dynamics and not just those of the seal or bearing alone. For a simulated bearing Prof. M.J. Braun of the University of Akron, Akron, Ohio, in a private communication has demonstrated that zones of secondary flow exist in the inlet and exit regions of a bearing such that the average fluid velocity is a minimum near the minimum gap.

From these results it is apparent that, although some average set of dynamic coefficients may be found, the three-dimensional effects are significant and local variations in these coefficients must be properly factored into an analysis.

5. CORRESPONDING STATES

This final section could also be entitled "similitudes that are useful to design and guides for experimentation." In most high-performance turbomachine applications the pressure gradients are sufficiently large to achieve sonic velocities (refs. 1 and 2). The principles of corresponding states have been applied to single- and multicomponent fluids and to single- and two-phase choked flows through venturis and through single and sequential Borda and orifice configurations (refs. 1, 9, 11, and 12). The principles have also been applied to regions of annular flows as found for example in bearings and seals (refs. 4 and 13 to 16). Reduced mass flux data for three space shuttle main engine (SSME) seal configurations for the cryogens nitrogen and hydrogen (refs. 13 to 15) tend to verify extending the principles of corresponding states to other fluids such as oxygen. However, for the extensions to include gaseous helium, the reduced helium pressure must be further normalized by a factor of 10 (fig. 7). At this time the reason for the factor of 10 is undetermined.

5

6. SUMMARY OF RESULTS

Herein we have discussed an approach to calculating flow and dynamic characteristics for seals or bearings. For the restricted model considered, the results are in reasonable agreement with a run selected from the data of Childs (ref. 3).

We discussed leakage rates and relations between pressure profiles and direct stiffness for three seal configurations of the space shuttle main engine class and related these profiles to postulated zones of secondary flow or separation. For these tests the seals were eccentric but the shaft was not rotating. Fluid injection was found to augment direct stiffness. Flow choking can occur within a seal. Within stepped configurations choking diverted the flow and effected a crossover in the pressure profiles within the upstream step, thereby decreasing direct stiffness (the same comment applies to the straight cylindrical seal). For a labyrinth seal carryover diminished from the entrance and effected a crossover in the pressure profiles within each of the three steps. As such, the direct stiffness changed from positive to negative.

Pressure measurements taken at 0° and 180° along the axial length of a seal or bearing are insufficient to define maximimum-to-minimum pressure variations and zones of secondary flows. This points out the need for careful instrumentation guided by three-dimensional computations, data, and intuition.

The local average velocity within a bearing or a seal emerged as the key to stability and was strongly influenced by inlet and exit effects and fluid injection, which in turn drove zones of secondary flow. Thus although some average set of dynamic coefficients may be found, the three-dimensional effects were significant and local variations in these coefficients must be properly integrated into an analysis.

The principles of corresponding states have been applied to seal and bearing flows and were found to be useful.

7. REFERENCES

1. Childs, D.W., Vance, J.M., and Hendricks, R.C., Eds. Rotordynamic Instability Problems in High-Performance Turbomachinery. NASA CP-2133, 1980; NASA CP-2250, 1982; NASA CP-2338, 1984; NASA CP-2443, 1986.

2. Bently, D.E., Muszynska, A., and Hendricks, R.C., Eds. Instability in Rotating Machinery. NASA CP-2409, 1986.

3. Childs, D.W. SSME HPFTP Interstage Seals: Analysis and Experiments for Leakage and Reaction-Force Coefficients. NASA CR-170876, 1983.

4. Hendricks, R.C. Some Flow Characteristics of Conventional and Tapered High-Pressure-Drop Simulated Seals, ASLE PREPRINT 79-LC-3B-2, 1979.

5. Braun, M.J., Hendricks, R.C., and Mullen, R.L. Studies of Two-Phase Flow in Hydrostatic Journal Bearings. In: Cavitation and Multiphase Flow Forum - 1984. New York:ASME 1984.

6. Mullen, R.L. and Hendricks, R.C. Finite Element Formulation for Transient Heat Treat Problems. In: ASME/JSME Thermal Engineering Conference, Proceedings, Vol. 3. New York:ASME 1984.

7. Tam, L.T. An Interim Report on the Calculation Method for a Multi-Dimensional Whirling Seal. CHAM 4010/7, CHAM, Huntsville, AL, 1985.

8. Hendricks, R.C. and Stetz, T.T. 1983. Studies of Flows Through N-Sequential Orifices. J. Fluids Eng. 105:297-302.

9. Hendricks, R.C. and Stetz, T.T. Some Flow Phenomena Associated with Aligned Sequential Apertures with Borda Type Inlets. NASA TP-1792, 1981.

10. Muszynska, A. Fluid-Related Rotor/Bearing/Seal Instability Problems. Bently Rotor Dynamics Research Corp., Minden NV 1986.

11. Simoneau, R.J. and Hendricks, R.C. Two-Phase Choked Flow of Cryogenic Fluids in Converging-Diverging Nozzles. NASA TP-1484, 1979.

12. Hendricks, R.C., Sengers, J.V. and Simoneau, R.J. Toward the Use of Similarity in Two-Phase Choked Flows. In: Scaling in Two-Phase Flows. New York:ASME 1980.

13. Hendricks, R.C. Straight Cylindrical Seal for High-Performance Turbomachines. NASA TP-1848, 1987.

14. Hendricks, R.C. Three-Step Cylindrical Seal for High-Performance Turbomachines. NASA TP-1849, 1987.

15. Hendricks, R.C. Three-Step Labyrinth Seal for High-Performance Turbomachines. NASA TP-1850, 1987.

16. Braun, M.J., Wheeler, R.L. and Hendricks, R.C. Thermal Shaft Effects on Load Carrying Capacity of a Fully Coupled, Variable Properties, Cryogenic Journal Bearing. ASLE Paper 86-TC-6B-1, 1986.

$$F_\varphi = (k_{xy} - C\omega)$$

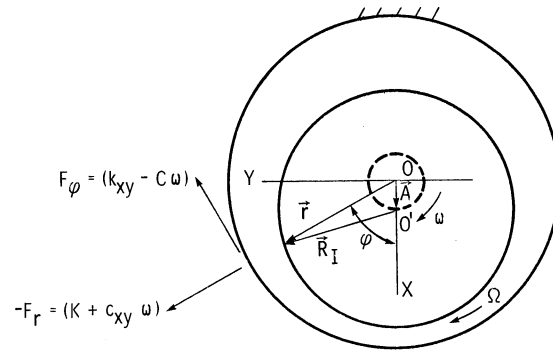$$-F_r = (K + c_{xy}\,\omega)$$

Figure 1. - Schematic of simulated stepped-seal configuration in a constant-Z plane.
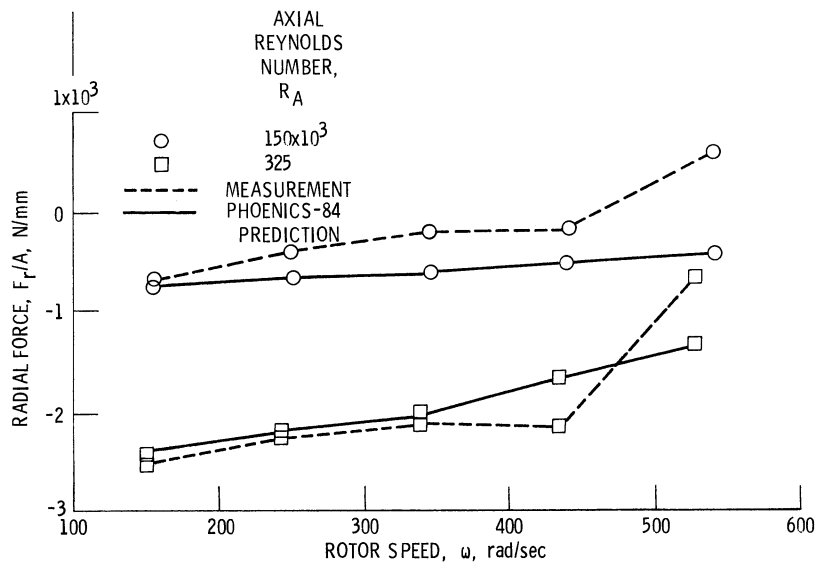

Figure 2. - Radial force as function of rotor speed for two axial Reynolds numbers. Stepped-seal data of Childs (ref. 3). (Herein $\omega = \Omega$.)
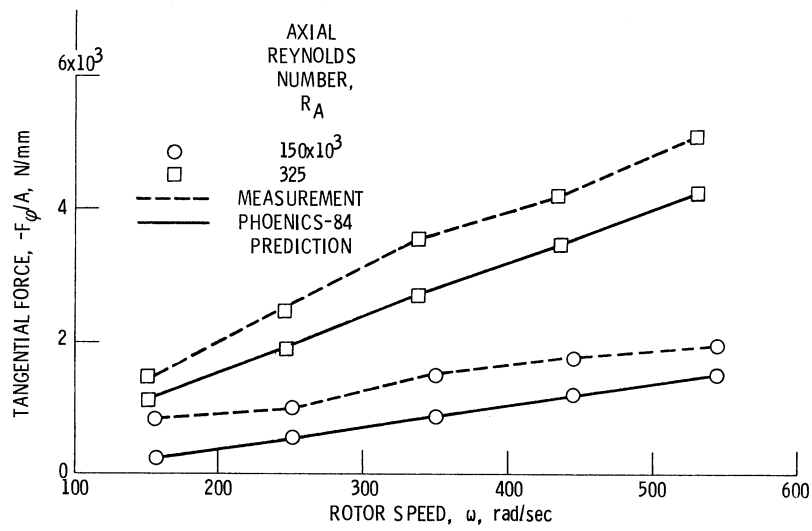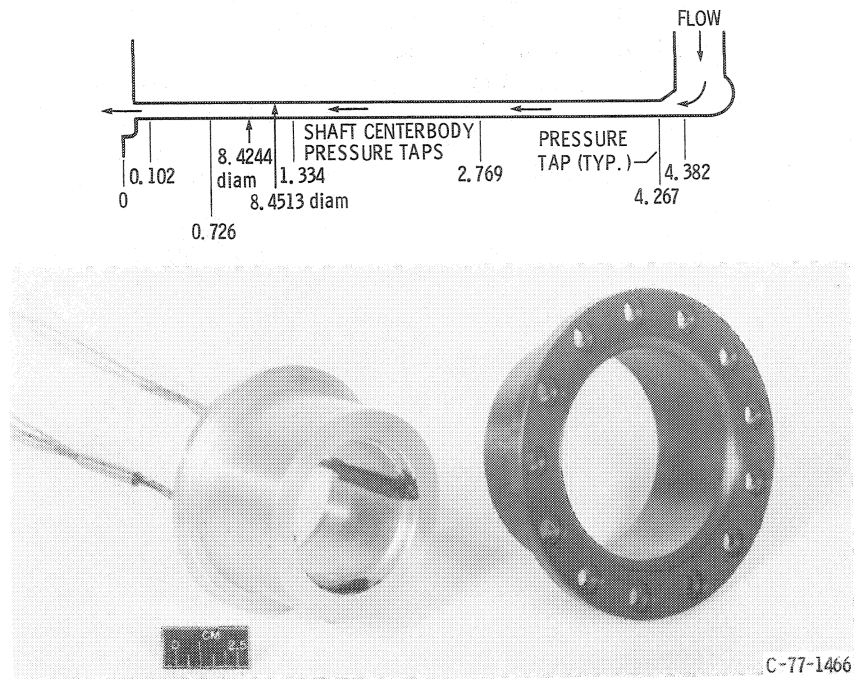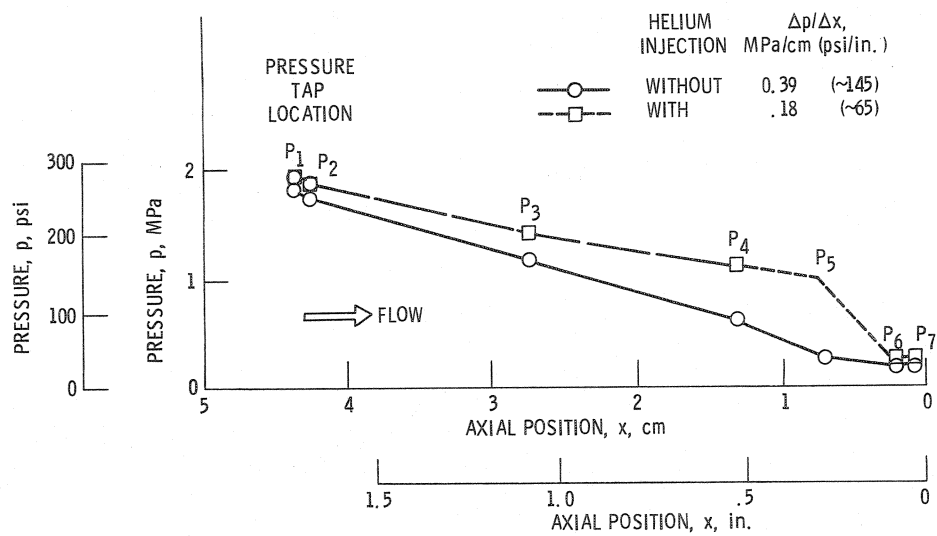
Figure 3. - Tangential force as function of rotor speed for two axial Reynolds numbers. Stepped-seal data of Childs (ref. 3). Whirl frequency ratio,

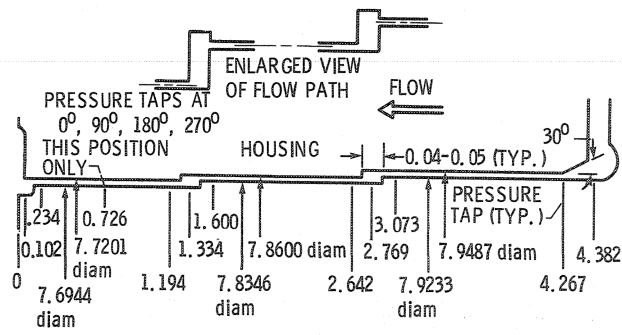$$k_{xy}/C\omega = 1 - \frac{-F_\varphi/A}{C\omega} < 1 \text{ as } \omega \text{ increases. (Herein } \omega = \Omega.)$$

FLOW

SHAFT CENTERBODY
PRESSURE TAPS

PRESSURE
TAP (TYP.)

8.4244 diam

8.4513 diam

| 0 | 0.102 | 0.726 | 1.334 | 2.769 | 4.267 | 4.382 |

C-77-1466

(a) Cylindrical shaft seal. (Dimensions are in centimeters.)

PRESSURE TAP LOCATION	HELIUM INJECTION	$\Delta p/\Delta x$, MPa/cm (psi/in.)	
—○—	WITHOUT	0.39	(~145)
--□--	WITH	.18	(~65)

P_1 P_2 P_3 P_4 P_5 P_6 P_7
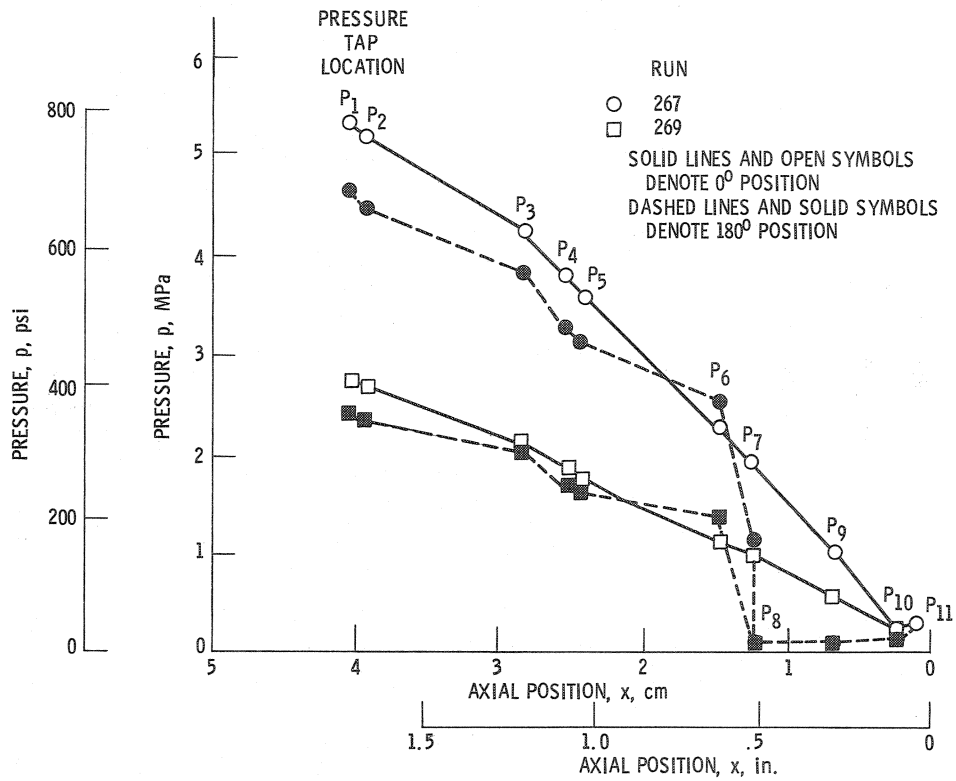
FLOW

PRESSURE, p, psi
PRESSURE, p, MPa
AXIAL POSITION, x, cm
AXIAL POSITION, x, in.

(b) Pressure profiles with and without fluid injection.

Figure 4. - Fluid injection into straight cylindrical seal.

ENLARGED VIEW
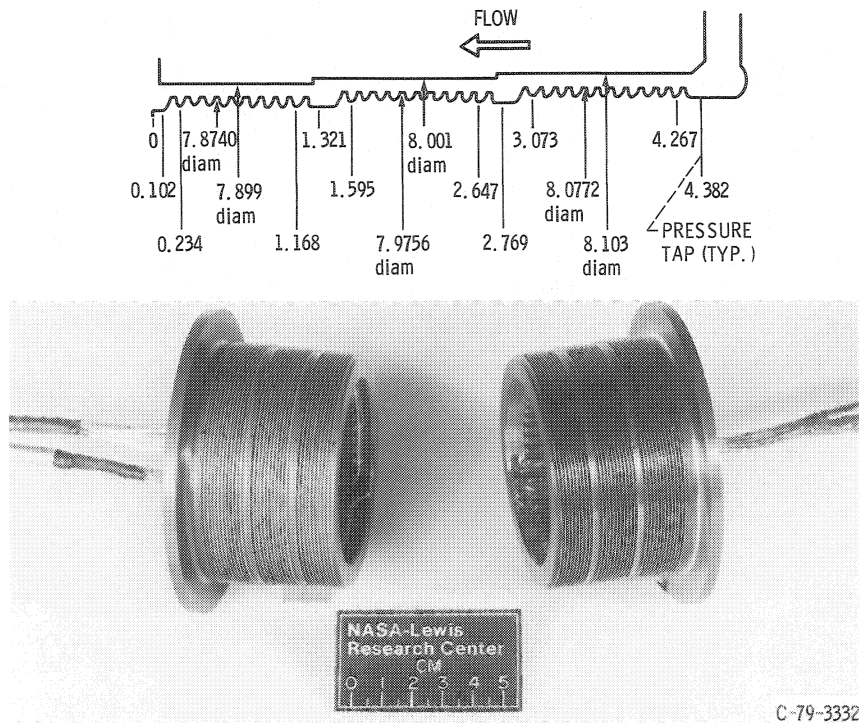OF FLOW PATH   FLOW

PRESSURE TAPS AT
0°, 90°, 180°, 270°
THIS POSITION   HOUSING   0.04-0.05 (TYP.)
ONLY   30°

PRESSURE
TAP (TYP.)

.234   0.726   1.600   3.073
0.102   7.7201   1.334   7.8600 diam   2.769   7.9487 diam   4.382
        diam
0   7.6944   1.194   7.8346   2.642   7.9233   4.267
        diam   diam   diam

(a) Three-step shaft seal configuration. (Dimensions are in centimeters.)
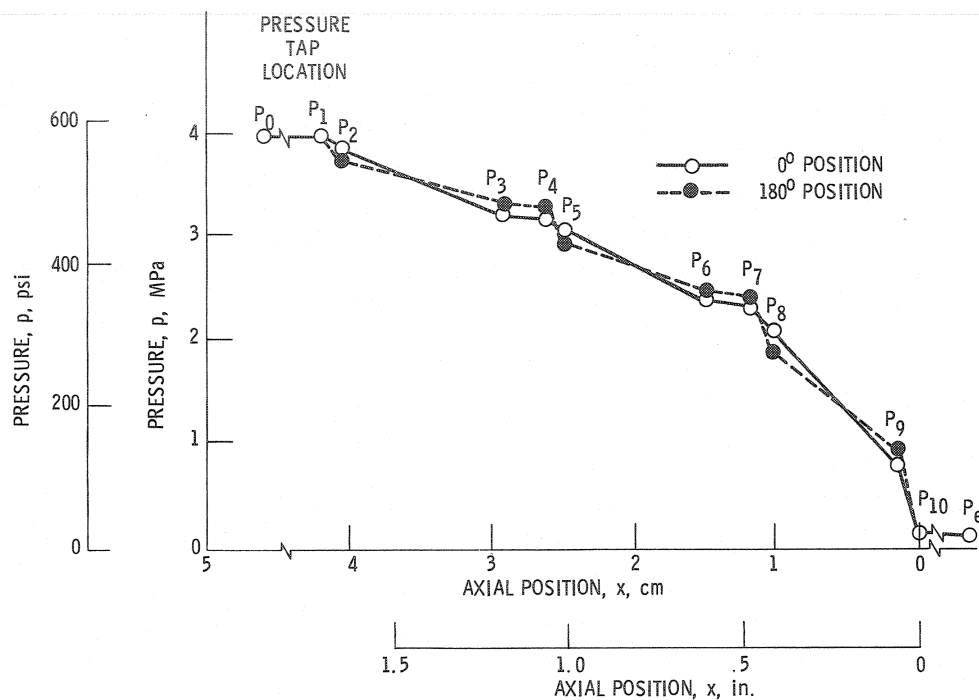

(b) Pressure profiles for fluid nitrogen with crossover and jetting; fully eccentric at 0°.

Figure 5. - Three-step cylindrical seal.

(a) 33-Tooth labyrinth shaft seal configuration. (Dimensions are in centimeters.)

(b) Pressure profiles for gaseous hydrogen with crossover; 2/3 fully eccentric position.
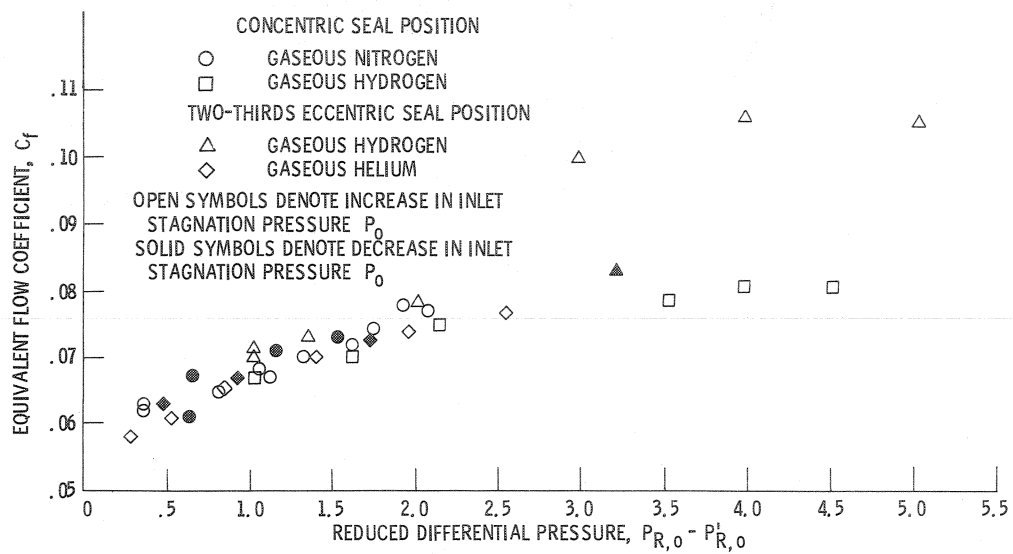
Figure 6. – Three-step labyrinth seal.

Figure 7. – Reduced mass flux as a function of reduced pressure differential for gases nitrogen, hydrogen, and helium flowing through a straight cylindrical seal (see fig. 4).

1. Report No.	2. Government Accession No.	3. Recipient's Catalog No.
NASA TM-88919		

4. Title and Subtitle	5. Report Date
Evaluation of Seals for High-Performance Cryogenic Turbomachines	
	6. Performing Organization Code
	553-12-00

7. Author(s)	8. Performing Organization Report No.
R.C. Hendricks, L.T. Tam, M.J. Braun, and B.L. Vlcek	E-3348
	10. Work Unit No.

9. Performing Organization Name and Address	11. Contract or Grant No.
National Aeronautics and Space Administration Lewis Research Center Cleveland, Ohio 44135	
	13. Type of Report and Period Covered

12. Sponsoring Agency Name and Address	Technical Memorandum
National Aeronautics and Space Administration Washington, D.C. 20546	14. Sponsoring Agency Code

16. Abstract

An approach to computing flow and dynamic characteristics for seals or bearings is discussed. The local average velocity was strongly influenced by inlet and exit effects and fluid injection, which in turn drove zones of secondary flow. For the restricted three-dimensional model considered, the integral averaged results were in reasonable agreement with selected data. Unidirectional pressure measurements alone were insufficient to define such flow variations. However, for seal and bearing leakage correlations the principles of corresponding states were found to be useful. Also discussed are three phenomena encountered during testing of three eccentric nonrotating seal configurations for the Space Shuttle Main Engine (SSME) Program. Fluid injection, choking within a seal, and pressure profile crossover are related to postulated zones of secondary flow or separation and to direct stiffness.

17. Key Words (Suggested by Author(s))	18. Distribution Statement
Seals; Rotordynamics; Fluid flow; Cryogenics; Turbomachines	Unclassified - unlimited STAR Category 34

19. Security Classif. (of this report)	20. Security Classif. (of this page)	21. No. of pages	22. Price*
Unclassified	Unclassified		

*For sale by the National Technical Information Service, Springfield, Virginia 22161